UNIVERSITÀ DEGLI STUDI FIRENZE

DISEI
DIPARTIMENTO DI SCIENZE PER L'ECONOMIA E L'IMPRESA

Working Papers – Economics

Eluding the Predators: the Goodwin Cycle with Workforce Precarization in Japan

Corrado Di Guilmi, Enrico Caricchio

Working Paper N. 18/2026

DISEI, Università degli Studi di Firenze
Via delle Pandette 9, 50127 Firenze (Italia)
www.disei.unifi.it

Eluding the predators: the Goodwin cycle with workforce precarization in Japan

Corrado Di Guilmi[1,2,3,4] and Enrico Caricchio[1]

[1] *University of Florence, Italy*
[2] *University of Technology Sydney, Australia*
[3] *Center for Computational Social Science, Kobe University, Japan*
[4] *Centre for Applied Macroeconomic Analysis, Australian National University, Canberra, Australia*

July 7, 2026

Abstract

This paper examines the implications of introducing non-regular workers, typically characterized by limited wage bargaining power, into the Goodwin cyclical growth framework, and applies the extended model to the Japanese data. Analytically, we incorporate this duality by adding a third dynamic equation to the original two-dimensional Goodwin system, assuming that firms turn to this secondary workforce to offset upward pressure on the wage share during periods of labor market tightness. The resulting three-dimensional system is studied empirically, analytically, and numerically. This threefold analysis reveals that the introduction of secondary workers substantially modifies the dynamics of class conflict and, under certain conditions, replaces the Goodwin limit cycle with a convergent equilibrium. Our empirical estimates suggest that Japanese firms' hiring behavior is consistent with the convergent regime. However, adjustment frictions in the composition of employment may slow the reallocation of workers across contract types, preventing convergence and allowing the economy to remain on the Goodwin limit cycle.

Keywords: Goodwin model, non-regular employment, distributional conflict.
JEL codes: C62, E25, E32.

1 Introduction

In Goodwin's limit cycle model (1967), rising employment strengthens workers' bargaining power, compressing the profit share and thereby reducing investment, aggregate production, and ultimately employment. The long-run growth of the economy is therefore characterized by a cyclical pattern whose evolution is driven by the distributive conflict between labor and capital. This cyclical growth pattern does not align with the general decline in the wage share observed across advanced capitalist economies, and in particular in Japan, over recent decades. To reconcile this empirical evidence with the predictions of the Goodwin model, we extend the theoretical framework to incorporate non-regular workers and apply the resulting model to the Japanese economy. Specifically, we examine whether firms' reliance on non-regular employment can moderate the increase in the wage share associated with declining unemployment, thereby disrupting the cyclical dynamics predicted by the Goodwin model.

The existing relevant literature extending the Goodwin model has focused on technological progress and financialization as possible avenues through which the capitalists can break or weaken the increase in wage share associated to a tight labor market (a full survey can be found in Barrales-Ruiz et al., 2022). Among the papers on induced productivity dynamics, Tavani and Zamparelli (2015) introduce endogenous technological change through Research and Development expenditure on labor augmenting innovation, showing that the model admits a stable steady state for a range of parameter values. In this case, the economy shows dampened oscillations, so that the dimension of the distributive conflicts gradually vanishes. They extend their results in Tavani and Zamparelli (2021), assuming that labor productivity growth is an increasing function of the wage share. In the same vein, Cajas Guijarro (2024) finds local stability by adding an endogenous supply of labor to the endogenous technical progress. Dosi et al. (2024) introduce a Kaldor-Verdoon increasing return specification for endogenous technical change, again showing that when the learning coefficient is high enough, the system becomes stable. In contrast, authors inspired by the seminal contribution by Chiarella and Flaschel (2000) study the interaction between the real and financial sides of the economy, using an extended Goodwin framework (see for example Asada et al., 2006; Di Guilmi et al., 2023; Franke et al., 2006).

We innovate with respect to this literature by focusing on the replacement of regular or primary workers with non-regular or secondary workers[1], characterized not only by lower wage but also by limited bargaining power. In fact Chen (2018); Fukao and Perugini (2021), among others, show that the precarization of the workforce and the associated erosion of workers' bargaining power are key factors in explaining the downward trend in the wage share in Japan (see Stansbury and Summers, 2020, for a similar argument relative the US). Fur-

[1]We adopt the Japan Standard Occupational Classification, 5^{th} revision, referring to regular employment (primary workers) as open-ended, full-time, direct employment, and to non-regular employment (secondary workers) as part-time workers, temporary workers, dispatched workers, contract employees, and entrusted employees.

thermore, Di Guilmi and Fujiwara (2022) and Hosono et al. (2014) find that financial constraints can lead firms to prefer secondary workers, who are typically cheaper and easier to layoff, over standard and more productive employees, when deciding about hiring. In line with these findings, Aoyama et al. (2022) argue that the increase in the use of secondary workers substantially contributed to the flattening of the Japanese Phillips curve observed from the year 2000. Sasaki et al. (2024) study the Goodwin cycle in dual labor market in Japan. Differently from the present study, their duality refers to skilled and unskilled workers and their focus is on the effects of the introduction of a minimum wage. As mentioned above, our concern is the duality in the type of contracts as it directly affects the bargaining power of workers and hence one of the crucial transmission mechanisms in Goodwin's story.

The novel question addressed in this paper is investigated through the close integration of empirical, analytical, and numerical approaches. Specifically, we examine the Goodwin cycle in Japan over the period 1984–2024 and study its relationship with the dynamics of the share of primary workers. We begin by estimating a linear approximation of the standard two-dimensional Goodwin model and then extend it by introducing a third equation describing the evolution of the relative shares of the two types of workers. To complement this investigation, we perform a cointegration analysis for the post–bubble and pre-COVID period. We then develop a theoretical model that builds on the basic Goodwin framework and derive its stability conditions. Finally, we calibrate the theoretical model using the estimated empirical parameters and conduct a numerical analysis that both extends and unifies the empirical and theoretical findings.

The threefold analysis shows that workers' contractual heterogeneity modifies the dynamics of class conflict and, under certain conditions, replaces the Goodwin limit cycle with a convergent equilibrium. Specifically, we assume that firms' hiring decisions depend on both the employment rate and the wage share. The stability and numerical analyses identify a quantitative condition linking the relative sensitivity of firms to these two variables, which determines whether the system converges to equilibrium. Our empirical estimates suggest that Japanese firms' hiring behavior is consistent with the convergent regime. However, adjustment frictions in the composition of employment may slow the reallocation of workers across contract types, preventing convergence and allowing the economy to remain on the Goodwin limit cycle.

The remainder of the paper is structured as follows. Section 2 presents the results of the empirical analysis of the Goodwin cycle, focusing on the dampening effect of the inclusion of a third variable that quantifies the employment contractual composition. Section 3 presents the extended Goodwin model, whose stability is discussed and detailed in section 4. Section 5 illustrates the results of the numerical simulations and section 6 concludes the paper with a discussion of the results.

2 Empirical evidence

This section illustrates the empirical results for the analysis of the standard and extended Goodwin model in Japan. Section 2.1 details the characteristics of the Goodwin cycles for the three time series on which we focus: employment rate, wage share, and share of regular workers. Section 2.2 explains the empirical strategy used to estimate the linearized Goodwin system. Finally sections 2.3 and 2.4 discuss the results for the estimations of, respectively, the standard and extended Goodwin systems.

2.1 Goodwin cycles in Japan

We use annual data for Japan covering the period 1984–2024. Quarterly data on workforce composition are available only from 2002 onward. We therefore rely on the annual data to examine the long-run dynamics of the Goodwin cycle and use the quarterly sample (2002–2019) for the cointegration analysis. Restricting the latter to the pre-pandemic period also mitigates the effects of major structural breaks, such as those associated with the aftermath of the asset-price bubble and the lost decade, as well as the COVID-19 pandemic, which may compromise cointegration analysis. Employment and wage share data are drawn from the Federal Reserve of St Louis data, while data on the composition of the workforce are provided by the Labor Force Survey, released by the Japanese Ministry of Health, Labor and Welfare.

Figure 1 reports the time series of employment (as share of the workforce), wage share, and share of primary workers over total workers in Japan . Similar patterns can be observed for employment and wage share, with a decline up to the early 2000s, a stagnant phase until about 2015 and an upward trend in the latest period. The share of primary workers monotonically declines up to 2014 and remains substantially unchanged afterwards.[2]

On account of the characteristics of the raw time series and according to the standard practice in the empirical literature on the Goodwin cycle (see Tavani, 2012, for example), we filter the three time series using the Hodrick-Prescott filter. Given the monotonic trend component in the share of primary workers, we focus on its first differences. Figure 2 shows the standard Goodwin cycle for the filtered employment and wage share data. The two variables display a positive relationship during the post-bubble era and a joint decline, more sizable in employment, followed by a recovery, which is initially larger in employment and then sharper in the wage share. Further, two sub-cycles appear, one with high employment and high wage share at the beginning and at the end of the period considered, and another with low employment and low wage share in the central phase. The contour plot of the cycle with the three-dimensional projection given by the difference in the trend of primary workers' share reveals that, in general, positive differences are concentrated in the high employment-high wage share regime (figure 3).

[2]For a disaggregated analysis of the dynamics of the share of primary and secondary workers

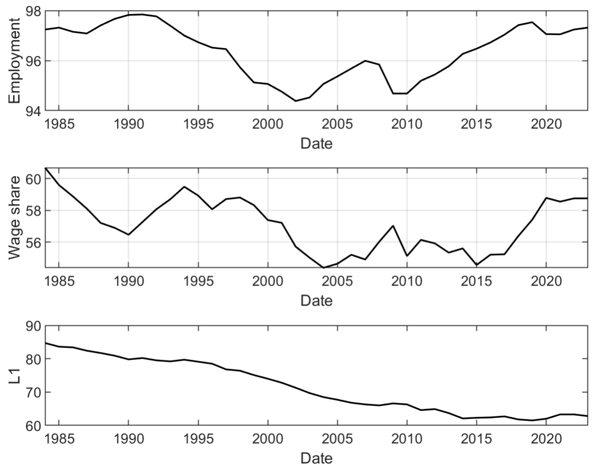

Figure 1: Employment, wage share, and share of primary workers in Japan

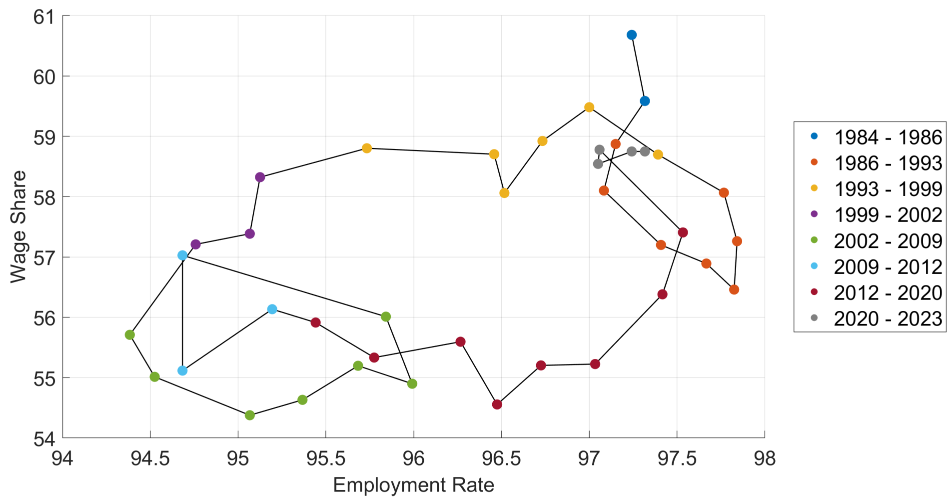

Figure 2: Japan Goodwin cycle

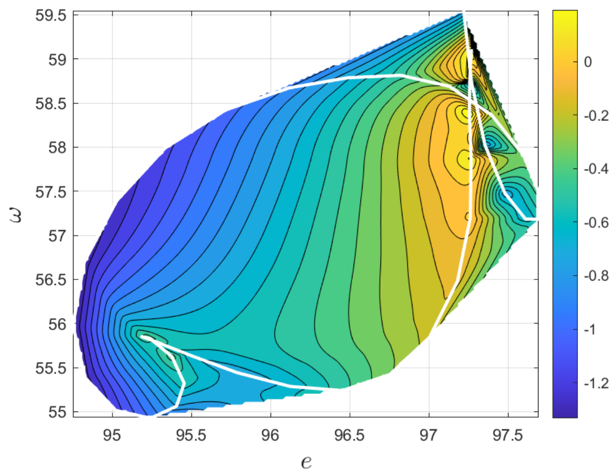

Figure 3: Japan cycle with change in share of primary workers

2.2 Empirical strategy

To study the empirical dynamics of the system, we estimate a linear approximation of the interaction between the employment rate and the wage share. The analysis is conducted both for the standard two-dimensional specification and for the extended three-dimensional model including the additional variable x, which, following Lux (1995), we define as the following relative index of the shares of the two types of workers:

$$x = l_1 - l_2 \tag{1}$$

with l_1 and l_2 the shares of primary and secondary workers respectively. Accordingly, x is bounded in $[-1, 1]$.

For the two-dimensional analysis, we linearly approximate the Goodwin system as

$$\Delta y_t = c + Ay_{t-1} + \varepsilon_t,$$

where A is the Jacobian matrix, c is the vector of intercepts, ε_t is error term, and

$$y_t = \begin{bmatrix} e_t \\ \omega_t \end{bmatrix},$$

where e_t is the employment rate, and ω_t is the wage share.

The coefficients of the system are estimated through multivariate ordinary least squares. In matrix form, the estimation problem is written as

$$Y = XB + U,$$

see Mizobata (2024).

where

$$Y = \begin{bmatrix} \Delta e_t & \Delta \omega_t \end{bmatrix},$$

and

$$X = \begin{bmatrix} 1 & e_{t-1} & \omega_{t-1} \end{bmatrix}.$$

The matrix U collects the regression residuals. The coefficient matrix is obtained as

$$B = (X'X)^{-1}X'Y.$$

The first row of B contains the intercept terms, while the remaining rows provide the coefficients associated with the lagged state variables. From estimated coefficients, we obtain the empirical Jacobian matrix

$$A = \begin{bmatrix} a_{11} & a_{12} \\ a_{21} & a_{22} \end{bmatrix}.$$

The empirical steady state is computed by imposing

$$\Delta y_t = 0,$$

which implies

$$Ay^* + c = 0.$$

Hence, the steady state vector is obtained as

$$y^* = -A^{-1}c.$$

The analysis is then extended to a three-dimensional specification including the variable x_t. In this case, the empirical system becomes

$$\Delta z_t = c + A_3 z_{t-1} + \varepsilon_t,$$

with

$$z_t = \begin{bmatrix} e_t \\ \omega_t \\ x_t \end{bmatrix}.$$

The corresponding 3×3 Jacobian matrix is estimated using the same procedure described above. The eigenvalues of the extended system are then used to evaluate the effect of the additional variable on the stability and convergence properties of the dynamics. Since the available sample is relatively short, the analysis focuses on local dynamic properties rather than on the estimation of a full vector autoregressive model.

2.3 Two-dimensional dynamics

The estimated two-dimensional Jacobian matrix is:

$$A = \begin{bmatrix} 0.0917 & -0.1383 \\ 0.3458 & -0.2047 \end{bmatrix}.$$

The sign structure of the matrix is consistent with the Goodwin mechanism. The negative coefficient of the wage share in the employment equation captures the classical profit-squeeze effect: higher wage shares reduce profitability and therefore dampens employment growth. Conversely, the positive coefficient of employment in the wage-share equation reflects a Phillips-curve mechanism whereby tighter labor markets strengthen workers' bargaining power and increase the wage share.

The empirical steady state of the system is

$$(e^*, \omega^*) = (96.39,\ 56.99),$$

The eigenvalues of the Jacobian matrix are:

$$\lambda_{1,2} = -0.0565 \pm 0.1608i.$$

The presence of complex eigenvalues indicates cyclical dynamics, while the negative real part implies that the cycles are damped over time. The economy therefore converges towards the steady state through oscillatory adjustments. Relative to the canonical Goodwin model, which generates closed orbits with purely imaginary eigenvalues, the empirical evidence suggests that the Japanese economy is characterized by persistent but ultimately convergent distributional cycles.

2.4 Three-dimensional extension

Adding the third equation for Δx as linear function of the three state variables, the estimated Jacobian matrix becomes

$$A_3 = \begin{bmatrix} 0.1164 & -0.1443 & -0.0376 \\ 0.1079 & -0.1476 & 0.3614 \\ 0.2158 & -0.1824 & -0.1015 \end{bmatrix}. \tag{2}$$

The coefficients associated with Δx in the first two equations suggest that labour-market composition influences both employment and distributional dynamics. In particular, changes in labor-market composition appear to have a negative short-run effect on employment growth and a positive effect on the evolution of the wage share. The introduction of this additional variable therefore enriches the transmission mechanisms of the model without altering its fundamental cyclical structure.

The corresponding empirical steady state is

$$(e^*, \omega^*, \Delta x^*) = (0.9561,\ 0.5636,\ -0.0113).$$

The first two components remain essentially unchanged relative to the two-dimensional specification, while the steady-state value of Δx is approximately zero.

The eigenvalues of the 3D system are

$$\lambda_1 = -0.0542,$$

and

$$\lambda_{2,3} = -0.0392 \pm 0.2642i.$$

All eigenvalues possess negative real parts, implying local stability of the equilibrium. The complex pair indicates that cyclical interactions between employment and income distribution remain the dominant source of fluctuations. Relative to the two-dimensional system, the imaginary part is somewhat larger, suggesting slightly more pronounced cyclical behavior, while the negative real part ensures convergence towards the steady state. The additional real eigenvalue is also negative and of similar magnitude to the real part of the complex pair.

To gain further insights about the influence of employment composition on the Goodwin cycle, it is useful to exclude the bubble-lost decade and the COVID periods, in which massive shocks impacted the job market. Quarterly data are available for the share of primary workers from 2002, and accordingly we focus on the period 2002-2019.[3] The eigenvalues become:

$$\lambda_{1,2} = -0.0643 - 0.2183i$$

and

$$\lambda_3 = -0.0825 + 0.0000i.$$

The variable x increases local stability by making the real parts of the dominant eigenvalues more negative while the imaginary part disappears altogether, signalling a convergent dynamics to a stable fixed point.

To test the role of employment composition in fundamentally altering the dynamics of the growth cycle, we estimate Johansen cointegration tests, focusing at first only on the employment rate and the wage share, and subsequently on the extended specification that includes the relative employment composition x. Table 1 reports the results for the bivariate system. The trace statistic fails to reject the null hypothesis of no cointegration at conventional significance levels. Hence, the data do not provide evidence of a stable long-run equilibrium relationship between employment and wage share alone.

The results change when x is included. As shown in Table 2, the null hypothesis of no cointegration is rejected at the 5% significance level, while the null of at most one cointegrating vector cannot be rejected. The extended system therefore exhibits a unique long-run equilibrium relationship.

[3] Di Guilmi and Rylah (2026) identify a structural shock that tilts the Beveridge curve in the Japanese labor market at the end of 2019, therefore right before the onset of the pandemic and at the end of the period of observation.

Null hypothesis	Trace statistic	Critical value (5%)	p-value
$r = 0$	13.9531	20.2619	0.3276
$r \leq 1$	3.0269	9.1644	0.6289

Table 1: Johansen trace test: employment rate and wage share.

Null hypothesis	Trace statistic	Critical value (5%)	p-value
$r = 0$	36.1127	35.1929	0.0397
$r \leq 1$	11.0719	20.2619	0.5680
$r \leq 2$	2.6805	9.1644	0.6809

Table 2: Johansen trace test: employment rate, wage share, and employment composition.

To assess the adjustment dynamics, we examine the estimated loading coefficients of the VECM. The adjustment matrix reported in table 3, which indicates that all three variables respond to deviations from the long-run equilibrium.

Variable	Loading coefficient
e	-0.0486
ω	-0.1810
x	-0.2439

Table 3: Estimated adjustment coefficients.

The employment composition index x exhibits the largest adjustment coefficient in absolute value, suggesting that it bears a substantial share of the burden of restoring equilibrium following a disturbance. Although the relatively limited sample size warrants caution in interpreting the magnitude of these coefficients, the evidence suggests a potential role of secondary employment in reducing the bargaining power of workers and therefore lead to the stabilization of the employment-distribution dynamics.

3 Model

This section presents first the assumptions for the standard two-dimensional Goodwin model and then the three-dimensional model, extended by adding workers' contract heterogeneity.

3.1 Goodwin model

Our workhorse is the standard Goodwin model with fixed coefficient production function given by:

$$Y = min(\sigma K, aL) \tag{3}$$

where K and L are the quantity of capital and labor, respectively, and $\sigma, a > 0$. Assuming perfectly elastic supply of labor and full capacity utilization, $Y = \sigma K = aL$. The wage share is quantified by $\omega = \frac{wL}{aL} = \frac{w}{a}$, (where w is the real wage). Accordingly, the profit share is given by $\pi = 1 - \omega$, while the profit rate is $\nu = \frac{Y(1-\omega)}{K} = \sigma(1-\omega)$. Since only capitalists save, growth and accumulation are determined by the profit share.

Growth rates for labor productivity and population are constant and exogenous and are given by α and n, respectively.

The reactivity of wages to employment is determined by the Phillips curve:

$$\frac{\dot{\omega}}{\omega} = -\phi_0 + \phi_1 e - \alpha \tag{4}$$

with $\phi_0 \geq 0,\ \phi_1 > 0$

Accordingly, the joint evolution of employment rate and wage share is given by the following system:

$$\dot{e} = \left[\frac{1-\omega}{\sigma} - (\alpha + n)\right] e(1-e) \tag{5}$$

$$\dot{\omega} = \left[\phi_1 e - (\alpha + \phi_0)\right] \omega(1-\omega) \tag{6}$$

The system has the standard Goodwin structure except for the logistic correction, which, following Galanis (2025) ensures meaningful values for e and ω, without imposing the modifications in the structure of the model proposed by Desai et al. (2006).

The system has two steady-state solutions:

- $e = \omega = 0$, which is uninteresting;
- $e^* = \frac{\alpha+\phi_0}{\phi_1}$, $\omega^* = 1 - \sigma(\alpha + n)$, which we can use for a graphical analysis.

Figure 4 provides a visual representation of the dynamics generated by the two-dimensional system. In order to match the empirical steady state $e = 0.96$, $\omega = 0.57$, the parameters are estimated as $\alpha = 0.0825$, $\phi_1 = 0.085938$. The population rate of growth is set equal to the actual average of the period 1984-2024 as $n = 0.09$, while the initial conditions are $e_0 = 0.94, \omega_0 = 0.6$, equal the actual ones in 1984. The other parameters are calibrated as $\sigma = 4$, $\phi_0 = 0$.[4]

3.2 Extension with secondary workers

Let us denote with L_1,L_2 the levels of primary workers and secondary workers respectively, and with the already introduced l_1 and l_2 their shares on the total employment level. The firms' hiring can be framed as a standard discrete-choice problem under uncertainty and incomplete information, which we treat following the estabilished literature sprung from the seminal works by Brock

[4]Since in the stability presented in section 4, we set $\phi_0 = 0$ and $\alpha_0 =$ (introduced later) to simplify the analysis, for consistency we keep the same setting in the numerical simulations.

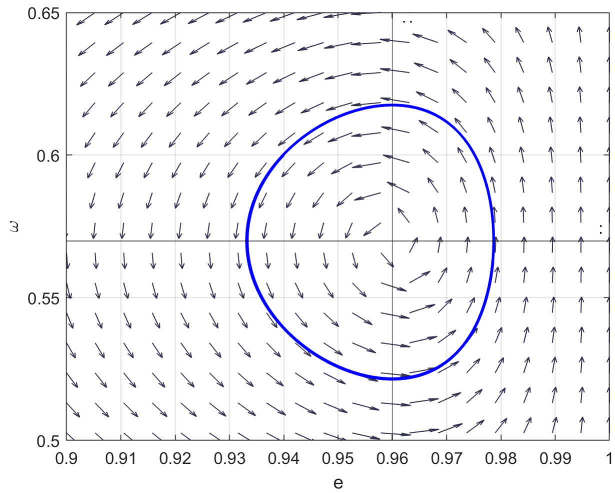

Figure 4: Phase diagram of the baseline model

and Hommes (1997); Lux (1995); Train (2009). We assume that the probability of hiring a primary worker increases with the level of employment, and therefore with the tightness of the labor market. As reported by the Ministry of Health, Labour and Welfare in a 2020 white paper, in a tight labor market, shortages concern mostly primary workers, and firms may resort to hire secondary workers in regular positions. In contrast, a higher wage share increases the probability of hiring a secondary worker as a cost-cutting device (Di Guilmi and Fujiwara, 2022; Hosono et al., 2014). Accordingly, for each hiring, the probability of a firm choosing a permanent worker is assumed to be

$$P_1 = \frac{e^{\beta_v}}{1 + e^{\beta_v}} \tag{7}$$

where

$$\beta_v = \beta_e e - \beta_\omega \omega, \tag{8}$$

and $\beta_e, \beta_\omega > 0$.

Given managerial and regulatory constraints, firms are unlikely to adjust the composition of their workforce instantaneously. Instead, hiring decisions are implemented only gradually. We model this adjustment friction by introducing the parameter $k \in (0, 1)$, where smaller values correspond to greater persistence in workforce composition. Accordingly, the evolution of the relative shares of workers is given by:

$$\dot{l}_1 = k\Big[(1 - l_1)P_1 - l_1(1 - P_1)\Big] = k(P_1 - l_1), \tag{9}$$

$$\dot{l}_2 = k(P_2 - l_2) = k\Big[(1 - P_1) - (1 - l_1)\Big], \tag{10}$$

respectively. Consequently, we can express the variation in the index of employment composition x, defined in equation (1), as:

$$\dot{x} = \dot{l}_1 - \dot{l}_2 = k\Big[2P_1 - x - 1\Big]. \tag{11}$$

According to the empirical literature, the introduction of secondary workers reduces both productivity (Fukao and Ug Kwon, 2006; Shinada, 2011) and bargaining power (Chen, 2018; Fukao and Perugini, 2021). Consequently, we reformulate the dynamics of both variables as follows:

$$\dot{\omega} = -\phi_0 + \phi_1 e x \tag{12}$$
$$\dot{a} = \alpha_0 + \alpha_1 x \tag{13}$$

Finally, the non-linear 3-dimensional system is given by:

$$\dot{e} = \left[\frac{1-\omega}{\sigma} - (\alpha_0 + \alpha_1 x) - n\right] e(1-e), \tag{14}$$
$$\dot{\omega} = \Big[-\phi_0 + \phi_1 e x - (\alpha_0 + \alpha_1 x)\Big]\omega(1-\omega), \tag{15}$$
$$\dot{x} = k\left(2\frac{e^{\beta_v}}{1+e^{\beta_v}} - x - 1\right), \tag{16}$$

The phase diagram for the three-dimensional model is presented, together with the parameter estimation, in section 5.

4 Stability analysis

We present here the results of the stability analysis, first illustrating the conditions for the existence of the fixed points and then discussing their stability.

4.1 Fixed Point Existence

To check whether an interior fixed point can be identified for meaningful values of the variables, we set $\dot{\omega} = \dot{e} = \dot{x} = 0$. Equation (16) becomes:

$$\frac{2e^{\beta v}}{1+e^{\beta v}} - x - 1 = 0$$

which cannot be solved in closed form. However, by imposing the steady state condition on equations (14) and (15), we obtain $\frac{1-\omega}{\sigma} - (\alpha_0 + \alpha_1 x) - n = 0$ and $-\phi_0 + \phi e x - (\alpha_0 + \alpha_1 x) = 0$, respectively. Accordingly, we can derive:

$$e(x) = \frac{\phi_0 + \alpha_0 + \alpha_1 x}{\phi_1 x} \tag{17}$$
$$\omega(x) = 1 - \sigma\left(\alpha_0 + \alpha_1 x + n\right) \tag{18}$$

and

$$\beta v(x) = \beta_e e(x) - \beta_\omega \omega(x) \tag{19}$$

Let us define the function $F : (-1, 1) \to \mathbb{R}$ as:

$$F(x) = \frac{2e^{\beta v(x)}}{1 + e^{\beta v(x)}} - x - 1 \tag{20}$$

so that $\dot{x} = 0$ if and only if $F(x) = 0$.
Further, the interior fixed point, if any, lies in $(0,1) \times (0,1) \times (-1,1)$, which implies that $e(x) = \frac{\phi_0+\alpha_0+\alpha_1 x}{\phi_1 x} < 1$ that is $x > \frac{\phi_0+\alpha_0}{\phi_1-\alpha_1} = \bar{x}$.
If $\phi_1 > \alpha_1 + \phi_0 + \alpha_0 > \alpha_1$ then $0 < \bar{x} < 1$ Furthermore, since $\phi_1 > \alpha_1 + \phi_0 + \alpha_0$ implies $\phi_1 > \alpha_1$, we can consider a restriction of F in the interval $(\bar{x}, 1) \subseteq (0, 1)$ i.e. $F : (\bar{x}, 1) \to \mathbb{R}$. As a result, we can identify the condition of existence of the fixed point according to proposition 1.

Proposition 1. *If* $\beta_e > \beta_\omega - \frac{\phi_1\sigma\beta_\omega(\phi_0+\alpha_0)+\alpha_1\sigma\beta_\omega(\phi_0+n)}{\phi_1-\alpha_1} + \frac{2(\alpha_0+\phi_0)(\phi_1-\alpha_1)}{(\phi_1-\alpha_1)^2-(\alpha_0+\phi_0)^2}$ *and* $\phi_1 > \alpha_1 + \phi_0 + \alpha_0$ *then* $x^* \in (\bar{x}, 1)$ *exists, with* $F(x^*) = 0$

Proof. See Appendix A □

From Proposition 1, we also obtain the following result for ω^*:

Remark 1. *Once* x^* *is determined under the condition of Proposition 1, then* $e^* = e(x^*)$ *and* $\omega^* = \omega(x^*)$ *are uniquely determined by 17 and 18 respectively. Moreover, if* $\frac{1}{\sigma} > \alpha_0 + \alpha_1 + n$*, then* $\omega^* \in (0, 1)$.

As a further result of Proposition 1 and Remark 1, we can state the following proposition:

Proposition 2 (Fixed Point Existence)**.** *If* $\beta_e > \beta_\omega - \frac{\phi_1\sigma\beta_\omega(\phi_0+\alpha_0)+\alpha_1\sigma\beta_\omega(\phi_0+n)}{\phi_1-\alpha_1} + \frac{2(\alpha_0+\phi_0)(\phi_1-\alpha_1)}{(\phi_1-\alpha_1)^2-(\alpha_0+\phi_0)^2}$,
$\phi_1 > \alpha_1 + \phi_0 + \alpha_0$ *and* $\frac{1}{\sigma} > \alpha_0 + \alpha_1 + n$ *then* $\omega^* \in (0, 1)$*. Then at least one interior fixed point* $(e^*, \omega^*, x^*) \in (0,1) \times (0,1) \times (\bar{x}, 1)$ *exists*

Proof. The proof follows directly form Proposition 1 and Remark 1 □

We can further note that in the fixed point x^*, when it exists, is always positive.

4.2 Stability

The Jacobian of the three-dimensional system in the fixed point is expressed by:

$$J^* = \begin{bmatrix} 0 & -\frac{e^*(1-e^*)}{\sigma} & -\alpha_1 e^*(1-e^*) \\ \phi_1 x^* \omega^*(1-\omega^*) & 0 & (\phi_1 e^* - \alpha_1)\omega^*(1-\omega^*) \\ k\frac{2e^{\beta v^*}}{(1+e^{\beta v^*})^2}\beta_e & -k\frac{2e^{\beta v^*}}{(1+e^{\beta v^*})^2}\beta_\omega & -k \end{bmatrix} \tag{21}$$

Let us define $A = e^* (1 - e^*)$, $B = \omega^* (1 - \omega^*)$ and $C = \frac{2e^{\beta v^*}}{\left(1+e^{\beta v^*}\right)^2}$.
Furthermore, given the interior fixed point (e^*, ω^*, x^*), for every values α_1, ϕ_1,β_e,β_ω,β_x, we can define:

$$k_0 := \frac{AB \left[\beta_e \left(\phi_1 e^* - \alpha_1\right)/\sigma - \beta_\omega \phi_1 \alpha_1 x^*\right]}{\beta_e \alpha_1 A + \beta_\omega (\phi_1 e^* - \alpha_1) B} \tag{22}$$

Since the denominator of k_0 is positive under the existence condition stated in Proposition 1, we have that $k_0 > 0$ if and only if $\beta_e \left(\phi_1 e^* - \alpha_1\right)/\sigma - \beta_\omega \phi_1 \alpha_1 x^* > 0$, i.e. $\beta_e > \frac{\beta_\omega \sigma \phi_1 \alpha_1 x^*}{(\phi_1 e^* - \alpha_1)}$.
In order for the condition in Proposition 2 to hold, it must be true that:
$\beta_e > \max\left\{\frac{\beta_\omega \sigma \phi_1 \alpha_1}{\phi_0 + \alpha_0}, \beta_\omega - \frac{\phi_1 \sigma \beta_\omega (\phi_0 + \alpha_0) + \alpha_1 \sigma \beta_\omega (\phi_0 + n) + \beta_x (\phi_0 + \alpha_0)}{\phi_1 - \alpha_1} + \frac{2(\alpha_0 + \phi_0)(\phi_1 - \alpha_1)}{(\phi_1 - \alpha_1)^2 - (\alpha_0 + \phi_0)^2}\right\} := \bar{\beta}_e$.
Hence, if $\beta_e > \bar{\beta}_e$, the interior fixed point exists and $k_0 > 0$. Accordingly, the stability condition for the fixed point can be stated as in Proposition 3

Proposition 3. *If $k > k_0$ the interior fixed point (e^*, ω^*, x^*) is locally asymptotically stable. At $k = k_0$ the system undergoes an Hopf bifurcation and a limit cycle arises.*

Proof. See Appendix B. □

5 Numerical analysis

This section presents the results of the numerical analysis of the extended three-dimensional system. In particular we focus first on the estimation of the three parameters that determine the evolution of the shares of regular and non-regular workers, and then we discuss the global sensitivity analysis on all the parameters.

5.1 Parameter estimation

The estimated Jacobian (2) provides useful information for calibrating the behavioural parameters of the extended model. Using the steady-state restriction implied by the sentiment equation together with the third row of the Jacobian we can estimate the parameters involved in equation (11).

Since $J(3,3) = -k$, from (2), we immediately obtain $\hat{k} = 0.1015$. To estimate β_e and β_ω, from (2), we can verify that:

$$\frac{J(3,1)}{J(3,2)} = \frac{\beta_e}{\beta_\omega} \tag{23}$$

Additionally, the steady state of (11) implies

$$0 = k\left(\frac{2e^{v^*}}{1 + e^{v^*}} - x^* - 1\right),$$

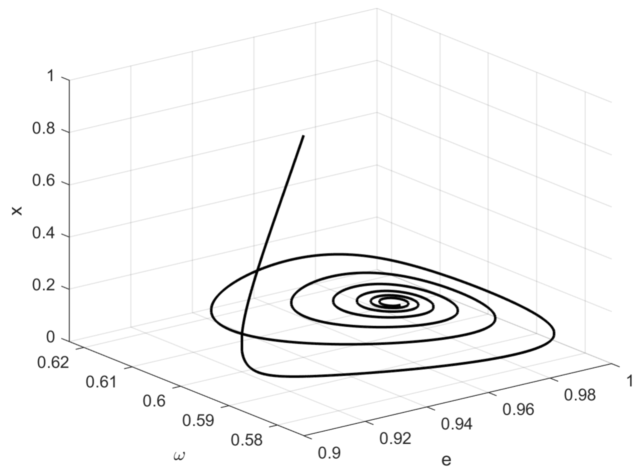

Figure 5: 3D phase diagram with dual labor market

with

$$v^* = \beta_e e^* - \beta_\omega \omega^*.$$

Since $k > 0$, it must be true that:

$$\frac{2e^{v^*}}{1 + e^{v^*}} - x^* - 1 = 0.$$

This gives

$$v^* = \log\left(\frac{1 + x^*}{1 - x^*}\right).$$

Therefore

$$\beta_e e^* - \beta_\omega \omega^* = \log\left(\frac{1 + x^*}{1 - x^*}\right) \tag{24}$$

Finally, (23) and (24) can be jointly used to estimate β_e and β_ω. The estimates for the three parameters are then:

$$\hat{\beta_e} = 0.5118, \hat{\beta_\omega} = 0.4326, \hat{k} = 0.1015.$$

These estimates imply that labour-market sentiment responds positively to employment conditions and negatively to increases in the wage share, consistently with our assumptions in (8). The joint dynamics of the three variables with the estimated parameters is displayed by figure 5, with all the parameters are set as for figure 4, with $\alpha_0 = 0$.

5.2 Global sensitivity analysis

To integrate the stability analysis and provide additional insights, we carry on a global sensitivity analysis on the main parameters. More specifically, a latin hypercube is built by sampling the parameter space in the ranges reported in table 4 and 100 combinations of the 5 parameters are drawn. For each simulation, we first look at the eigenvalues to evaluate whether the fixed points are locally stable or unstable, then we take the maximum Lyapunov exponent for the subset of unstable points. The maximum Lyapunov exponent is quantified for each combination of the parameters are plotted in figures 6-8. We classify the results as interior stable (green points) if the fixed point is inside the interval $(0, 1)$ for all the three variables; stable (orange) if the fixed point identify a corner solution (either 0 or 1 for one of the variables); limit cycle (purple); chaos (red). The white areas indicate combinations for which a fixed point cannot be identified. The resulting values of the Lyapunov exponent are therefore robust to the parametrization and allows for more general conclusions than a simple univariate bifurcation analysis.

Figure 6 shows the results for β_e and β_ω, which are of particular interest since they feature in the behavioral equation that we add to the standard Goodwin system. The results are in line with the analytical findings, which identify a threshold of β_e for the system to be stable. Furthermore, the plot identifies a particular ratio β_e/β_ω for which an interior stable fixed point emerges. This outcome is in line with the Jacobian (21) since $\frac{J(3,1)}{J(3,2)} = \frac{\beta_e}{\beta_\omega}$ and therefore the stability of the system depends on the relative magnitude of these parameters. Relatively large values of β_e imply a greater use of primary workers and thus conditions similar to the standard Goodwin model and the emergence of a limit cycle. In contrast, a large β_ω pushes firms to hire more secondary workers with ambiguous effects since the increase in the profit share is counterbalanced by a decline in productivity.

We also report in the plot the values for the two parameters estimated following the procedure illustrated in the previous subsection. Admittedly, the result must be taken with a grain of salt as it is based on a linear approximation of the system. However, the estimation lies within the stable area, confirming the results of the econometric analysis that suggest that a stabilizing effect due to the missed increase in bargaining power normally associated with a raising employment might be at work in Japan.

Figure 7 reveals that this stabilizing effect might be hindered by a too-slow adjustment in workforce composition. For low values of k (including the value of 0.1015 estimated on the Japanese data) the system remains trapped in a limit cycle, with a reduced influence from β_e and β_ω.

Figure 8 completes the illustration of the results by showing the combination of the three main parameters determining x with the other two parameters that interact with the composition of the workforce. In general it is possible to appreciate that larger ϕ_1, by increasing the sensitivity of the wage share to employment and therefore the bargaining power of workers, lead to a limit cycle, while a higher α_1, by increasing labor productivity and thus tilting distribution

Parameter	Range
ϕ_1	$[0.01, 1]$
α_1	$[0.01, 1]$
β_e	$[0.01, 2.0]$
β_ω	$[0.01, 2.0]$
k	$[0.01, 0.25]$

Table 4: Parameter range for global sensitivity analysis.

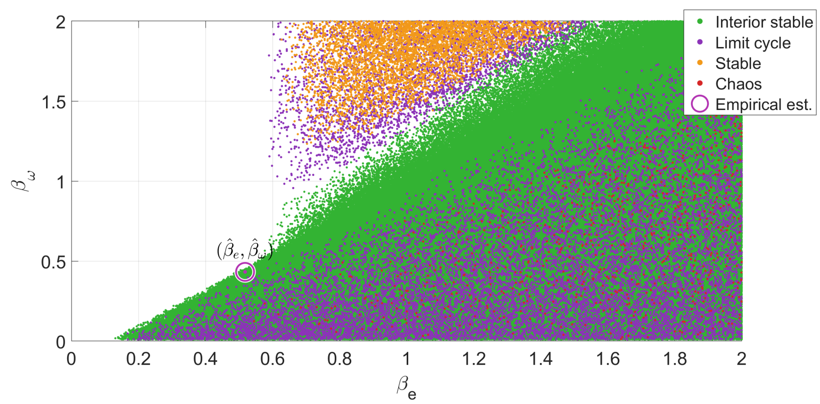

Figure 6: Lyapunov exponent analysis for β_e, β_ω.

towards profits, is more likely to generate a stable equilibrium.

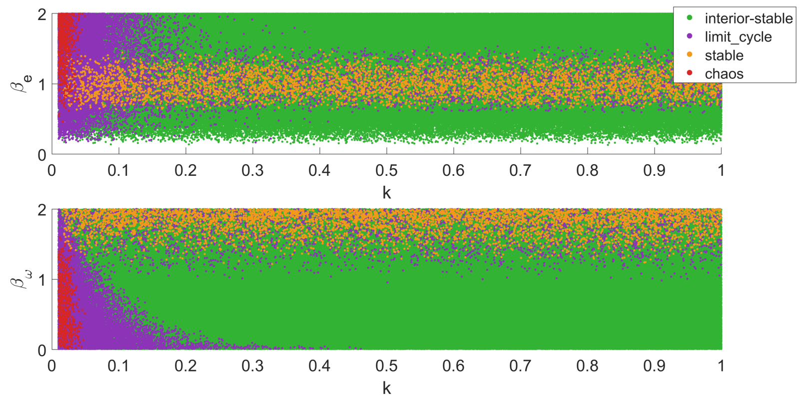

Figure 7: Lyapunov exponent analysis for for k, β_e, β_ω.

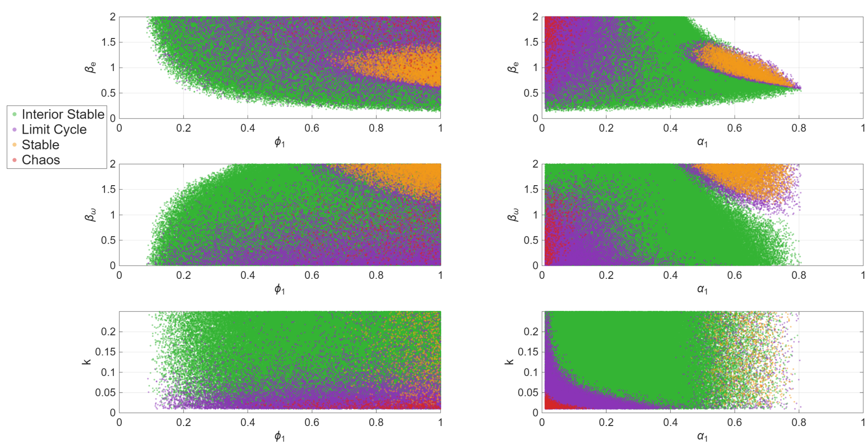

Figure 8: Lyapunov exponent analysis for $k, \beta_e, \beta_\omega, \phi_1, \phi_0$.

6 Discussion and concluding remarks

Despite the limitations due to the number of observations, the joint interpretation of the empirical, analytical, and numerical results sheds light on the main question that we set out to answer. The possibility of firms to resort to non-regular employment has had a dampening effect on the Goodwin cycle, especially from the 2000s, suggesting that firms can partially relax the distributive pressures generated by tight labour markets through greater reliance on non-regular employment. This conclusion is supported by three results. The first is the sign of the real part of the eigenvector of the three-dimensional linearized dynamical system estimated on the data, and the null imaginary component estimated for the period 2022-2019. The second is the output of the cointegration analysis for the post-2000 data. The Johansen tests and the estimation of the error correction coefficients of the VECM jointly point to the employment composition as stabilizing factor in the cyclical dynamics. The third result is given by the empirically estimated coefficients that measure the sensitivity of firms to employment and wage share in the theoretical model, which lie in the ranges that lead a convergent equilibrium (Figure 6). Let us clarify that stabilization here does imply an improvement in macroeconomic performance due to smoother business cycles. Rather, it corresponds to the suppression of distributive dynamics through weaker wage adjustment, resulting in the possibility of a persistent combination of relatively high employment and stagnant labor income. In this sense, the disappearance of Goodwin-type cycles does not reflect the emergence of a more balanced growth regime.

In fact, these results suggest that the empirically verified weakening of bargaining power of workers due to the increase in non-regular employment allows for a contemporaneous raise in employment and decline or stagnation in wage share, thus preventing transition to the contractionary phase in the Goodwin cycle. This interpretation also provides a structural explanation for the flattening of the wage Phillips curve documented for Japan. As already proposed in the theoretical analysis by Aoyama et al. (2022), the weakening of the wage-employment relationship may partly originate from employment arrangements that reduce workers' bargaining power.

Interestingly, the relatively low value estimated for the speed of adjustment in employment shares k suggests that, despite the underlying breaking up of the Goodwin cycle due to the unresponsiveness of the wage share to employment, the cycle may apparently survive because of the impossibility of swift changes in hiring strategies due to obvious constraints, both internal and external to the firms. Employment contracts, training costs, firm-specific human capital, legal constraints, and recruitment frictions all generate inertia in the transition between regular and non-regular employment. Consequently, although the structural mechanism weakens the distributive feedback underlying the Goodwin cycle, the gradual adjustment of employment composition may allow for oscillatory behavior to persist.

The results are consistent with the literature discussed in the introduction on labor market dualism, according to which firms increasingly rely on peripheral workers to increase numerical flexibility while limiting the bargaining power of core employees. In this perspective, non-regular employment affects macroeconomic dynamics not only through wage moderation but also by altering the feedback mechanism between employment and income distribution that lies at the core of the Goodwin cycle. The estimated dynamics are also consistent with the well-documented transformation of the Japanese labour market since the 1990s, characterized by the rapid expansion of non-regular employment, persistent wage stagnation, and declining union bargaining power. Rather than representing independent phenomena, our results suggest that these developments may be interpreted as mutually reinforcing elements of a single macroeconomic adjustment process.

Our findings complement and enrich the literature extending the Goodwin model to account for institutional and structural changes in labour markets. While previous contributions have mostly focused on productivity growth and financialization, our results suggest that changes in the composition of employment constitute an additional mechanism through which distributive conflict can be moderated. The composition of employment appears to influence not only the level of wages or employment but also the qualitative properties of macroeconomic dynamics, including the stability of equilibrium and the persistence of the cyclical growth pattern.

The results of this paper suggest possible future avenues for research in both Goodwin-type theoretical models, in particular to incorporate labor market heterogeneity, and empirical macro-labor analysis, for identifying the macroeconomic implications of the changes in distributive dynamics due to the modifications in labor contracts and labor market segmentation.

References

Aoyama, H., Di Guilmi, C., Fujiwara, Y., and Yoshikawa, H. (2022). Dual labor market and the phillips curve puzzle: the Japanese experience. *Journal of Evolutionary Economics*, 32(5):1419–1435.

Asada, T., Chen, P., Chiarella, C., and Flaschel, P. (2006). Keynesian dynamics and the wage-price spiral: A baseline disequilibrium model. *Journal of Macroeconomics*, 28(1):90–130.

Barrales-Ruiz, J., Mendieta-Muñoz, I., Rada, C., Tavani, D., and von Arnim, R. (2022). The distributive cycle: Evidence and current debates. *Journal of Economic Surveys*, 36(2):468–503.

Brock, W. and Hommes, C. (1997). A rational route to randomness. *Econometrica*, 65:1059–1095.

Cajas Guijarro, J. (2024). An extended Goodwin model with endogenous technical change and labor supply. *Structural Change and Economic Dynamics*, 70:699–710.

Chen, W. (2018). Upward wage rigidity and Japan's dispatched worker system. *Economic Modelling*, 73:152–162.

Chiarella, C. and Flaschel, P. (2000). *The Dynamics of Keynesian Monetary Growth: Macrofoundations.* Cambridge University Press, Cambridge.

Desai, M., Henry, B., Mosley, A., and Pemberton, M. (2006). A clarification of the Goodwin model of the growth cycle. *Journal of Economic Dynamics and Control*, 30(12):2661–2670.

Di Guilmi, C. and Fujiwara, Y. (2022). Dual labor market, financial fragility, and deflation in an agent-based model of the Japanese macroeconomy. *Journal of Economic Behavior and Organization*, 196:346–371.

Di Guilmi, C., Galanis, G., and Proaño, C. R. (2023). A baseline model of behavioral political cycles and macroeconomic fluctuations. *Journal of Economic Behavior & Organization*, 213(C):50–67.

Di Guilmi, C. and Rylah, G. K. (2026). Behind the curve: econometric estimation and sectoral decomposition of the Japanese Beveridge curve's evolution around the COVID-19 pandemic. *Industrial and Corporate Change*, 35(2):435–465.

Dosi, G., Usula, D., and Virgillito, M. E. (2024). Increasing returns and labor markets in a predator-prey model. *Journal of Evolutionary Economics*, 34(2):375–402.

Franke, R., Flaschel, P., and Proaño, C. R. (2006). Wage-price dynamics and income distribution in a semi-structural Keynes-Goodwin model. *Structural Change and Economic Dynamics*, 17(4):452–465.

Fukao, K. and Perugini, C. (2021). The long-run dynamics of the labor share in Japan. *Review of Income and Wealth*, 67(2):445–480.

Fukao, K. and Ug Kwon, H. (2006). Why did Japan's TFP growth slow down in the lost decade? An empirical analysis based on firm-level data of manufacturing firms. *The Japanese Economic Review*, 57(2):195–228.

Galanis, G. (2025). Unionization, distribution and macroeconomic dynamics. Technical report. mimeo.

Goodwin, R. M. (1967). A growth cycle. In Feinstein, C., editor, *Socialism, Capitalism and Economic Growth*, pages 54–58. Cambridge University Press, Cambridge.

Hosono, K., Takizawa, M., and Tsuru, K. (2014). The Impact of a Demand Shock on the Employment of Temporary Agency Workers: Evidence from Japan during the global financial crisis. Discussion papers 14046, Research Institute of Economy, Trade and Industry (RIETI).

Lux, T. (1995). Herd behaviour, bubbles and crashes. *Economic Journal*, 105:881–889.

Ministry of Health, Labour and Welfare (2020). Challenges facing japan: Work styles and labor shortages. *Japan Labor Issues*, 4(23):3–9. MHLW's White Paper on the Labor Economy 2019.

Mizobata, H. (2024). Japanâ€™s dual labor market and its macroeconomic characteristics. *Empirical Economics*, 67(1):165–196.

Sasaki, H., Asada, Y., and Sonoda, R. (2024). Effects of minimum wage share and wage gap reduction on cyclical fluctuation: A Goodwin approach. MPRA Paper 121695, University Library of Munich, Germany.

Shinada, N. (2011). Quality of Labor, Capital, and Productivity Growth in Japan: Effects of employee age, seniority, and capital vintage. Discussion papers 11036, Research Institute of Economy, Trade and Industry (RIETI).

Stansbury, A. and Summers, L. H. (2020). The declining worker power hypothesis: An explanation for the recent evolution of the american economy. *Brookings Papers on Economic Activity*, 51(1 (Spring)):1–96.

Tavani, D. (2012). Wage bargaining and induced technical change in a linear economy: Model and application to the US (1963–2003). *Structural Change and Economic Dynamics*, 23(2):117–126.

Tavani, D. and Zamparelli, L. (2015). Endogenous technical change, employment and distribution in the Goodwin model of the growth cycle. *Studies in Nonlinear Dynamics & Econometrics*, 19(2):209–216.

Tavani, D. and Zamparelli, L. (2021). Labor-augmenting technical change and the wage share: New microeconomic foundations. *Structural Change and Economic Dynamics*, 56:27–34.

Train, K. (2009). *Discrete Choice Methods with Simulation.* Cambridge University Press, Princeton.

Appendix A Proof Of Proposition 1

Proof. First, let us consider:

$$\begin{aligned}\lim_{x\to 1}\beta v(x) &= \lim_{x\to 1}\beta_e e - \beta_\omega \omega = \\ &= \frac{\beta_e\left(\phi_0+\alpha_0+\alpha_1\right)}{\phi_1} - \beta_\omega\left[1-\sigma\left(\alpha_0+\alpha_1+n\right)\right] = \overline{\beta v} \in \mathbb{R}\end{aligned}$$

so that:

$$\begin{aligned}\lim_{x\to 1}F(x) &= \lim_{x\to 1}\frac{2e^{\beta v(x))}}{1+e^{\beta v(x)}} - x - 1 \\ &= 2\left(\frac{e^{\overline{\beta v}}}{1+e^{\overline{\beta v}}} - 1\right) < 0,\end{aligned}$$

since $\frac{e^{\overline{\beta v}}}{1+e^{\overline{\beta v}}} < 1$ always.
Moreover

$$\begin{aligned}&\lim_{x\to \bar{x}}\beta_e e - \beta_\omega \omega = \\ &= \frac{\beta_e\left(\phi_0+\alpha_0+\alpha_1\bar{x}\right)}{\phi_1} - \beta_\omega\left[1-\sigma\left(\alpha_0+\alpha_1\bar{x}+n\right)\right] + \beta_x\bar{x} \\ &= \beta_e - \beta_\omega\left[1-\sigma\left(\alpha_0+\alpha_1\bar{x}+n\right)\right] = \underline{\beta v} \in \mathbb{R},\end{aligned}$$

so that:

$$\begin{aligned}\lim_{x\to \bar{x}}F(x) &= \lim_{x\to \bar{x}}\frac{2e^{\beta v(x))}}{1+e^{\beta v(x)}} - x - 1 \\ &= \frac{2e^{\underline{\beta v}}}{1+e^{\underline{\beta v}}} - \bar{x} - 1.\end{aligned}$$

Note that:

$$\frac{2e^{\underline{\beta v}}}{1+e^{\underline{\beta v}}} - \bar{x} - 1 > 0 \iff e^{\underline{\beta v}} > \frac{1+\bar{x}}{1-\bar{x}} \iff \underline{\beta v} > \ln\left(\frac{1+\bar{x}}{1-\bar{x}}.\right)$$

From the first order Taylor approximation of $\ln\left(\frac{1+\bar{x}}{1-\bar{x}}\right)$, it directly follows that: $\ln\left(\frac{1+\bar{x}}{1-\bar{x}}\right) < \frac{2\bar{x}}{1-\bar{x}^2}$. Expanding the last inequality and rearranging, we can write:

$$\beta_e - \beta_\omega + \frac{\phi_1\sigma\beta_\omega\left(\phi_0+\alpha_0\right)+\alpha_1\sigma\beta_\omega\left(\phi_0+n\right)+\beta_x\left(\phi_0+\alpha_0\right)}{\phi_1-\alpha_1} > \frac{2\left(\alpha_0+\phi_0\right)\left(\phi_1-\alpha_1\right)}{\left(\phi_1-\alpha_1\right)^2-\left(\alpha_0+\phi_0\right)^2}$$

which is true since we assume that:

$$\beta_e > \beta_\omega - \frac{\phi_1\sigma\beta_\omega\left(\phi_0+\alpha_0\right)+\alpha_1\sigma\beta_\omega\left(\phi_0+n\right)+\beta_x\left(\phi_0+\alpha_0\right)}{\phi_1-\alpha_1} + \frac{2\left(\alpha_0+\phi_0\right)\left(\phi_1-\alpha_1\right)}{\left(\phi_1-\alpha_1\right)^2-\left(\alpha_0+\phi_0\right)^2}$$

That proves that $\lim_{x\to\bar{x}}F(x) > 0$, and the proof can be completed by applying the Intermediate Value Theorem to $F(x)$ □

Appendix B Proof Of Proposition 3

Proof. In order to test the stability of the fixed point, we verify whether the Routh-Hurwitz conditions hold. Preliminarily, to simplify the notation, let us again use $A = e^*(1-e^*)$, $B = \omega^*(1-\omega^*)$ and $C = \frac{2e^{\beta v^*}}{\left(1+e^{\beta v^*}\right)^2}$. Accordingly, the Jacobian (21) becomes:

$$J^* = \begin{bmatrix} 0 & -\frac{A}{\sigma} & -\alpha_1 A \\ \phi_1 x^* B & 0 & (\phi_1 e^* - \alpha_1) B \\ k\beta_e C & -k\beta_\omega C & -k \end{bmatrix}$$

The characteristic equation associated to J^* is:

$$\lambda^3 + a_1\lambda^2 + a_2\lambda + a_3 = 0$$

with:

$$a_1 = -tr(J^*) = k$$

$$a_2 = \sum \textit{Principal minors of second order} = \frac{AB}{\sigma}\phi_1 x^* + kC\left[\alpha_1 A\beta_e + (\phi_1 e^* - \alpha_1) B\beta_\omega\right]$$

$$\begin{aligned} a_3 = -det(J^*) &= \frac{A}{\sigma}\left[\phi_1 x^* Bk + (\phi_1 e^* - \alpha_1) Bk\beta_e C\right] - \alpha_1\phi_1\beta_\omega x^* C \\ &= kAB\left[\frac{\phi_1 x^*}{\sigma} + \frac{\beta_e(\phi_1 e^* - \alpha_1) C}{\sigma} - \alpha_1\phi_1\beta_\omega x^* C\right] \\ &= \frac{kAB\phi_1 x^*}{\sigma} + kABC\left[\frac{\beta_e(\phi_1 e^* - \alpha_1)}{\sigma} - \beta_\omega\phi_1\alpha_1 x^*\right] \end{aligned}$$

We can verify that $a_1, a_2, a_3 > 0$, since each is a sum of positive terms. For a_1 and a_2 this is immediate. For a_3, its first term is manifestly positive, and its second term is positive because $\beta_e > \bar{\beta}_e$ implies

$$\beta_e > \frac{\sigma\beta_\omega\phi_1\alpha_1 x^*}{\phi_1 e^* - \alpha_1},$$

which in turn makes the expression in square brackets positive.

To verify the sufficient condition for stability, we construct the corresponding Routh array for the characteristic equation. The first two rows are populated directly from the polynomial coefficients, yielding Row 1: $[1, a_2]$ and Row 2: $[a_1, a_3]$. The first element of the third row (λ^1) is computed via the Routh cross-multiplication algorithm using the four elements directly above it: $\frac{(a_1\cdot a_2)-(1\cdot a_3)}{a_1} = \frac{a_1 a_2 - a_3}{a_1}$. According to the Routh-Hurwitz criterion, asymptotic stability requires all elements in the first column to be strictly positive. Given the necessary conditions $a_1 > 0$ and $a_3 > 0$, the requirement for the third row simplifies directly to the final sufficient condition: $a_1a_2 - a_3 > 0$. The full expression is developed as follows:

$$
\begin{aligned}
a_1a_2 - a_3 = k &\left[\frac{AB}{\sigma}\phi_1 x^* + kC\left(\beta_e\alpha_1 A + \left(\phi_1 e^* - \alpha_1\right) B\beta_\omega\right)\right] - \\
&- kAB\left[\frac{\phi_1 x^*}{\sigma} + \frac{\beta_e\left(\phi_1 e^* - \alpha_1\right) C}{\sigma} - \alpha_1\phi_1\beta_\omega x^* C\right] = \\
\\
&= k^2\left[\beta_e\alpha_1 A + \left(\phi_1 e^* - \alpha_1 B\beta_\omega\right)\right] - \frac{kAB\beta_e\left(\phi_1 e^* - \alpha_1\right) C}{\sigma} + kAB\alpha_1\phi_1\beta_\omega x^* C = \\
&= k\left[\beta_e\alpha_1 A + \left(\phi_1 e^* - \alpha_1 B\beta_\omega\right)\right] + AB\left[\alpha_1\phi_1\beta_\omega - \beta_e\left(\phi_1 e^* - \alpha_1\right)\right]
\end{aligned}
$$

From equation (22), it is possible to verify that the expression in the last row is positive, and therefore $a_1a_2 - a_3 > 0$, if and only if $k > k_0$. Hence, we have that, if $k > k_0$, for the Routh-Hurwitz criterion the fixed point is locally asymptotically stable.
Finally, we can investigate the behavior of the system for $k = k_0$. According to the Liu Theorem, a Hopf bifurcation occurs in $k = k_0$ if:

1. $\Delta_1 = a_{1|k_0} > 0$
2. $\frac{d}{dk}\left(a_1a_2 - a_3\right)_{|k_0} \neq 0$

The first condition is verified under our assumptions, since $\Delta_1 = a_{1|k_0} = k_0 > 0$. The full expression of the second condition is:

$$
\begin{aligned}
&\frac{d}{dk}\left(a_1a_2 - a_3\right)_{|k_0} = \\
\\
&= \frac{AB}{\sigma}x^* + k_0\left[\beta_e\alpha_1 A + \left(\phi_1 e^* - \alpha_1\right) B\beta_\omega\right] + k_0 C\left[\beta_e\alpha_1 A + \left(\phi_1 e^* - \alpha_1 B\beta_\omega\right)\right] + \\
&+ AB\left[-\frac{\phi_1 x^*}{\sigma} - \frac{\beta_e\left(\phi_1 e^* - \alpha_1\right)}{\sigma} + \alpha_1\phi_1\beta_\omega C\right] = \\
\\
&= C\overbrace{\left[k_0\left(\beta_e\alpha_1 A + \left(\phi_1 e^* - \alpha_1\right) B\beta_\omega\right) + AB\left(\alpha_1\phi_1\beta_\omega - \frac{\beta_e\left(\phi_1 e^* - \alpha_1\right)}{\sigma}\right)\right]}^{=0 \text{ by def of } k_0} + \\
&+ k_0\left[\beta_e\alpha_1 A + \left(\phi_1 e^* - \alpha_1\right) B\beta_\omega\right] = \\
\\
&= k_0\left[\beta_e\alpha_1 A + \left(\phi_1 e^* - \alpha_1\right) B\beta_\omega\right] > 0
\end{aligned}
\tag{25}
$$

The last row's inequality always holds if the fixed point exists, since $\beta_e > \bar{\beta}_e$ for Proposition 1. □